ChemPubSoc Europe

DOI: 10.1002/chem.201402803

CHEMISTRY
A European Journal
Full Paper

Silicon Coordination Chemistry

2-Acylpyrroles as Mono-anionic *O*,*N*-Chelating Ligands in Silicon Coordination Chemistry

Alexander Kämpfe,[a] Erica Brendler,[b] Edwin Kroke,[a] and Jörg Wagler*[a]

In memory of Prof. Daniel Kost

Abstract: Kryptopyrrole (2,4-dimethyl-3-ethylpyrrole) was acylated with, for example, benzoyl chloride to afford 2-benzoyl-3,5-dimethyl-4-ethylpyrrole (**L^{1}H**). With $SiCl_4$ this ligand reacts under liberation of HCl and formation of the complex **L$^1_2$SiCl$_2$**. In related reactions with $HSiCl_3$ or H_2SiCl_2, the same chlorosilicon complex is formed under liberation of HCl and H_2 or liberation of H_2, respectively. The chlorine atoms of **L$^1_2$SiCl$_2$** can be replaced by fluoride and triflate using ZnF_2 and Me_3Si-OTf, respectively. The use of a supporting base (triethylamine) is required for the complexation of phenyltrichlorosilane and diphenyldichlorosilane. The complexes **L$^1_2$SiCl$_2$**, **L$^1_2$SiF$_2$**, **L$^1_2$Si(OTf)$_2$**, **L$^1_2$SiPhCl**, and **L$^1_2$SiPh$_2$** exhibit various configurations of the octahedral silicon coordination spheres (i.e. *cis* or *trans* configuration of the monodentate substituents, different orientations of the bidentate chelating ligands relative to each other). Furthermore, cationic silicon complexes **L$^1_3$Si$^+$** and **L$^1_2$SiPh$^+$** were synthesized by chloride abstraction with $GaCl_3$. In contrast, reaction of **L$^1_2$SiCl$_2$** with a third equivalent of **L^{1}H** in the presence of excess triethylamine produced a charge-neutral hexacoordinate Si complex with a new tetradentate chelating ligand which formed by Si-templated C–C coupling of two ligands **L^1**.

Introduction

Among the great variety of silicon compounds with a hypercoordinate Si atom,[1,2] a large group of complexes have been synthesized with the aid of mono-anionic bidentate *O*,*N*-chelating ligands[3] (such as **I**, **II**, **III** and **IV**). Furthermore, silicon complexes with other ligand systems (such as in **V**, **VI** and **VII**) contain the pyrrolide moiety as an N-donor function of the ligand.[4] Surprisingly, silicon complexes with pyrrole-functionalized mono-anionic bidentate *O*,*N*-chelators have not been reported to date, even though a simple class of that kind of ligands, that is, 2-acylpyrroles, is accessible via convenient syntheses and has been investigated as the ligand moiety in various other coordination compounds of main group and transition metals.[5]

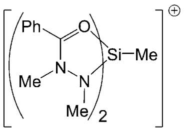

I

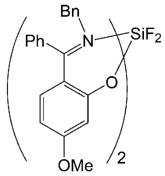

II

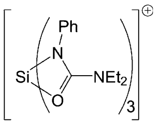

III

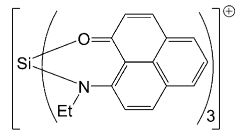

IV

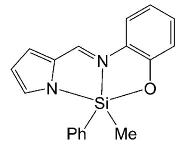

V

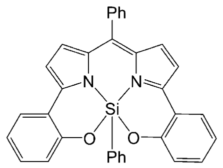

VI

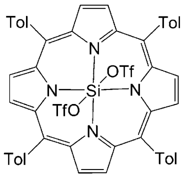

VII

In the course of our investigations, we have studied silicon complexes with bi-, tri-, and tetradentate *O*,*N*-donor ligands,[3b,c,f,4a,b,6] silicon complexes with five-membered *N*-heterocyclic donor moieties,[2g,h,7] and other silicon compounds of pyrrole-derived ligand systems.[8] In the work reported herein, we now address silicon complexes with pyrrole-functionalized bidentate *O*,*N*-chelating ligands.

Results and Discussion

Base-supported acylation of "kryptopyrrole" (2,4-dimethyl-3-ethylpyrrole) with acylchlorides provides easy access to various 2-acyl-3,5-dimethyl-4-ethyl-1*H*-pyrroles (e.g., ligands **L$^{1-4}$H**,

---

[a] Dipl.-Chem. A. Kämpfe, Prof. Dr. E. Kroke, Dr. J. Wagler
Institut für Anorganische Chemie
Technische Universität Bergakademie Freiberg
09596 Freiberg (Germany)
Fax: (+49) 3731394058
E-mail: joerg.wagler@chemie.tu-freiberg.de

[b] Dr. E. Brendler
Institut für Analytische Chemie
Technische Universität Bergakademie Freiberg
09596 Freiberg (Germany)

Supporting Information for this article is available on the WWW under http://dx.doi.org/10.1002/chem.201402803.

© 2014 Wiley-VCH Verlag GmbH & Co. KGaA, Weinheim

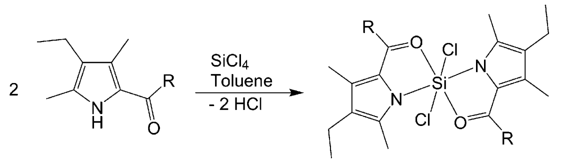

L^1H: R = Ph
L^2H: R = p-C_6H_4-NO_2
L^3H: R = p-C_6H_4-OMe
L^4H: R = 2-thienyl

$L^1{}_2SiCl_2$: R = Ph
$L^2{}_2SiCl_2$: R = p-C_6H_4-NO_2
$L^3{}_2SiCl_2$: R = p-C_6H_4-OMe
$L^4{}_2SiCl_2$: R = 2-thienyl

Scheme 1. Syntheses of hexacoordinate dichlorosilicon complexes with two chelating 2-acylpyrrolide ligands.

Scheme 1) as crystalline solids. The molecular structures of **L^1H**, **L^2H**, **L^3H**, and **L^4H** in the crystal are displayed in the Supporting Information. These compounds react with $SiCl_4$ under liberation of HCl, even in the absence of a supporting base (Scheme 1), to afford the hexacoordinate dichlorosilicon bischelates **$L^{1-4}{}_2SiCl_2$**, which precipitated from the reaction mixture as yellow powders that are poorly soluble in various organic solvents. Hexacoordination of their Si atoms was confirmed by ^{29}Si CP/MAS NMR spectroscopy ($\delta_{iso} = -171$ ppm in all cases). Crystals suitable for X-ray diffraction analyses were grown by slow reaction in undisturbed dilute solutions.

Thus, the molecular structures of compounds **$L^1{}_2SiCl_2$**, **$L^2{}_2SiCl_2$**, and **$L^4{}_2SiCl_2$** were determined by single-crystal X-ray diffraction analysis (Figure 1). In general, these complexes exhibit an *all-trans* configuration of their hexacoordinate Si coordination spheres and, due to the location of the Si atom on a center of inversion, 180° *trans* angles. Comparison of some selected bond features of these compounds reveals the subtle influence of the remote acyl substituent (R) on the Si coordination characteristics of the individual ligands. Along the series **$L^4{}_2SiCl_2$**, **$L^1{}_2SiCl_2$**, **$L^2{}_2SiCl_2$** (R = thienyl, phenyl, p-nitrophenyl) we observe a shortening of the Si–Cl bonds and a lengthening of the Si–O and Si–N bonds. These features of the Si coordination spheres and the shortening of the N1–C4 and O1–C9 bonds observed along the same series are indicators for the lowering of the ligand donor strength from R = thienyl via phenyl to p-nitrophenyl. As the ligand variation revealed only a subtle influence on the silicon coordination chemistry, we limited our further studies to complexes of the benzoyl-substituted ligand **L^1H**.

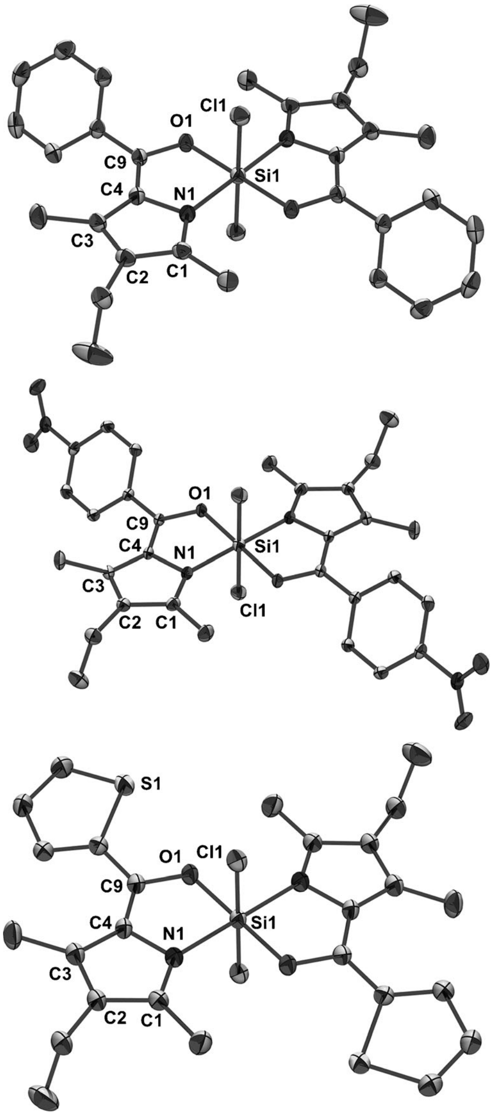

Figure 1. Molecular structures of (from top) **$L^1{}_2SiCl_2$**, **$L^2{}_2SiCl_2$**, and **$L^4{}_2SiCl_2$** in the crystal. Selected atoms are labelled and hydrogen atoms are omitted for clarity. In all cases the Si atom is located on a crystallographic center of inversion. Selected bond lengths [Å]: **$L^1{}_2SiCl_2$**: Si1–Cl1 2.228(1), Si1–O1 1.766(1), Si1–N1 1.875(2), N1–C4 1.409(3), C4–C9 1.381(3), O1–C9 1.325(2); **$L^2{}_2SiCl_2$** Si1–Cl1 2.219(1), Si1–O1 1.781(1), Si1–N1 1.887(2), N1–C4 1.400(2), C4–C9 1.388(3), O1–C9 1.311(2); **$L^4{}_2SiCl_2$** Si1–Cl1 2.241(1), Si1–O1 1.765(1), Si1–N1 1.863(2), N1–C4 1.411(2), C4–C9 1.385(3), O1–C9 1.323(2).

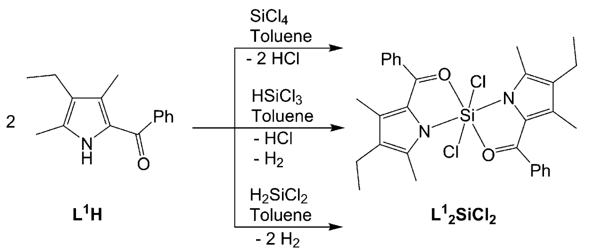

Scheme 2. Alternative synthesis routes of complex **$L^1{}_2SiCl_2$**.

In analogy to the reaction with $SiCl_4$ (see Scheme 1; yield 92%), ligand **L^1H** was treated with $HSiCl_3$ and H_2SiCl_2 in toluene, again in a 2:1 stoichiometric ratio (Scheme 2). Surprisingly, the same dichlorosilicon complex **$L^1{}_2SiCl_2$** formed in both cases and in similar yield (92% and 87%), as confirmed by ^{29}Si CP/MAS NMR spectroscopy and elemental analyses. Thus, dehydrogenative coupling must have taken place, as a combination of dismutation (into $SiCl_4$ and SiH_4) and chelation under HCl elimination would have caused yields below 75% or below 50% for the reactions with $HSiCl_3$ and H_2SiCl_2, respectively. Even though silicon complexation under H_2 elimination proved to be an elegant method for the preparation of hypercoordinate Si complexes,[9] this dehydrogenative coupling is particularly interesting because of the unsaturated ligand moieties involved, that is, the carbonyl function. As shown in previous studies, addition of Si–H bonds to unsaturated ligand moieties

© 2014 Wiley-VCH Verlag GmbH & Co. KGaA, Weinheim

(e.g., 1,3-H-transfer to imine C atoms[10] and 1,5-H-transfer to phenanthroline[11]) would provide an alternative reaction pathway, which has not been observed in the current case though.

Halide exchange in **L$^1_2$SiCl$_2$** with ZnF_2 (Scheme 3) afforded the difluorosilicon complex **L$^1_2$SiF$_2$**, which exhibited very good solubility in solvents such as THF and benzene, whereas the dichlorosilicon precursor was hardly soluble in various organic solvents. The ^{29}Si NMR spectra of this compound confirm silicon hexacoordination: In solution, a triplet ($^1J_{Si,F} = 181$ Hz) appears at $\delta = -170.9$ ppm, and in the CP/MAS spectrum a complex signal was observed at $\delta = -170$ ppm (see the Supporting Information), which resembles the signal shape of another hexacoordinate difluorosilicon-bis-chelate reported by Tacke et al.[12] Its signal characteristics can be attributed to dipolar coupling effects that arise from the *cis*-disposed Si–F bonds.[13] Single-crystal X-ray structure analysis of the benzene solvate of **L$^1_2$SiF$_2$** (Figure 2) revealed the configurational change of the silicon coordination sphere upon halide exchange, that is, transformation into a complex with *cis*-arranged halides. Similar behavior (*cis* SiF_2 vs. *trans* $SiCl_2$ moieties in related hexacoordinate silicon *O,N*-bis-chelates) has previously been reported for other ligands and has been attributed to the size difference of atoms in the Si coordination sphere Cl > O > F.[14] In the particular case of **L$^1_2$SiF$_2$**, the C1-bound methyl group thus causes less repulsion with the Si-bound F atom, whereas in an *all-trans* configuration related to **L$^1_2$SiCl$_2$** this methyl group would face the slightly larger O atom O1 of the opposite bidentate ligand, which would result in enhanced steric repulsion. The ligand arrangement of **L$^1_2$SiF$_2$** results in the O-donor atom being *trans*-disposed to the Si–F bond. Therefore, the stronger Si–F bond causes significant lengthening of the Si–O bond with respect to that in the precursor compound with a *trans* O-Si-O orientation (**L$^1_2$SiF$_2$** 1.842(1) vs. **L$^1_2$SiCl$_2$** 1.766(1) Å), whereas the still *trans*-oriented Si–N bonds show less response to the configurational change of the complex (**L$^1_2$SiF$_2$** 1.883(2) vs. **L$^1_2$SiCl$_2$** 1.875(2) Å). Si–O bond lengthening furthermore results in a shortening of the intra-ligand bond C9–O1 (**L$^1_2$SiCl$_2$** 1.325(2) vs. **L$^1_2$SiF$_2$** 1.309(2) Å).

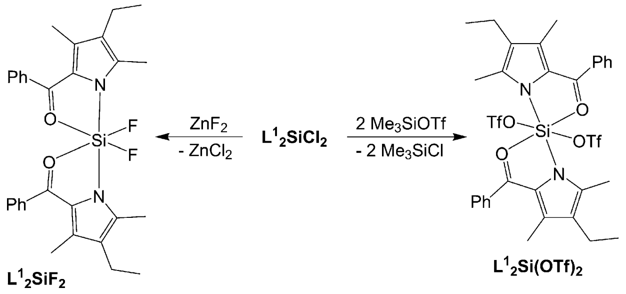

Scheme 3. Substitution of chloride in **L$^1_2$SiCl$_2$**.

A different effect on the silicon coordination sphere is observed upon replacing the Si-bound chlorine by the more ionic triflate (Scheme 3, Figure 2), which proceeds under retention of the *all-trans* configuration and which causes a similar shortening of both the Si–O and Si–N bonds to the bidentate ligands (**L$^1_2$SiCl$_2$** 1.766(1), 1.875(2) vs. **L$^1_2$Si(OTf)$_2$** 1.746(1), 1.842(1) Å, respectively). As expected, Si–O bond shortening causes a lengthening of the C9–O1 bond (to 1.331(1) Å).

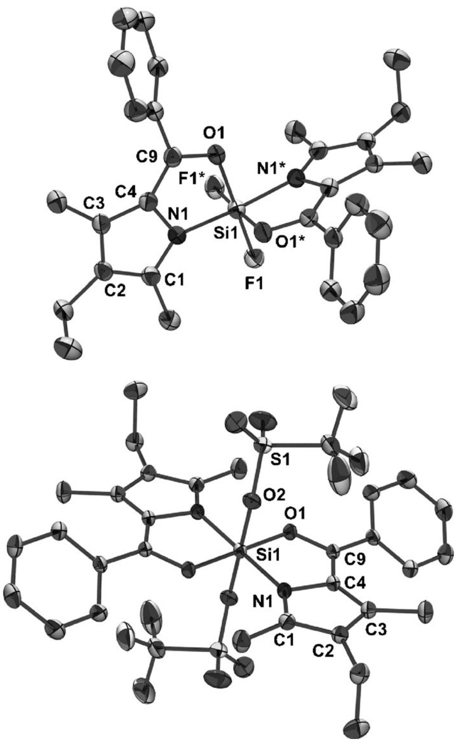

Figure 2. Molecular structures of (from top) **L$^1_2$SiF$_2$** and **L$^1_2$Si(OTf)$_2$** in the crystal. Selected atoms are labelled, hydrogen atoms and the solvent molecule of **L$^1_2$SiF$_2$ · C_6H_6** are omitted for clarity. The Si atom is located on a crystallographic twofold axis (in **L$^1_2$SiF$_2$**) or on a center of inversion (in **L$^1_2$Si(OTf)$_2$**). Selected bond lengths [Å] and angles [°]: **L$^1_2$SiF$_2$**: Si1–F1 1.632(1), Si1–O1 1.842(1), Si1–N1 1.883(2), N1–C4 1.403(3), C4–C9 1.386(3), O1–C9 1.309(2); F1-Si1-F1* 93.6(1), F1-Si1-O1 176.9(1), N1-Si1-N1* 165.4(1); **L$^1_2$Si(OTf)$_2$**: Si1–O1 1.746(1), Si1–O2 1.870(1), Si1–N1 1.842(1), N1–C4 1.411(1), C4–C9 1.383(2), O1–C9 1.331(1).

Whereas complexes of the type **L$_2$SiCl$_2$** were prepared without the aid of a sacrificial base (and further complexes could be derived by anion exchange reactions), phenylchlorosilanes exhibit significantly lower reactivity towards the 2-benzoylpyrrole ligand **L^{1}H**, that is, upon heating $PhSiCl_3$ and **L^{1}H** in toluene under reflux for 3 h the unreacted ligand was recovered as the sole solid, and $PhSiCl_3$ was the only silane detected by ^{29}Si NMR spectroscopy of the crude "reaction" solution. Base-supported substitution, using triethylamine as the base, was applied to successfully synthesize the *O,N*-bis-chelate complexes **L$^1_2$SiPhCl** and **L$^1_2$SiPh$_2$** from the corresponding chlorosilanes (Scheme 4).

In these hexacoordinate Si complexes we found the *all-trans* configuration for **L$^1_2$SiPhCl** in analogy to the dichlorosilicon complex, whereas **L$^1_2$SiPh$_2$** reveals an alternative configuration with *cis*-arranged monodentate groups and this time *trans*-disposed Si–O bonds (Figure 3). This particular configuration can be rationalized in a manner similar to that for the related configuration of **L$^1_2$SiF$_2$**, that is, the methyl groups in the pyrrole-2-position need to face the sterically least demanding substituent, which is the O atom of the chelating ligand. Whereas this

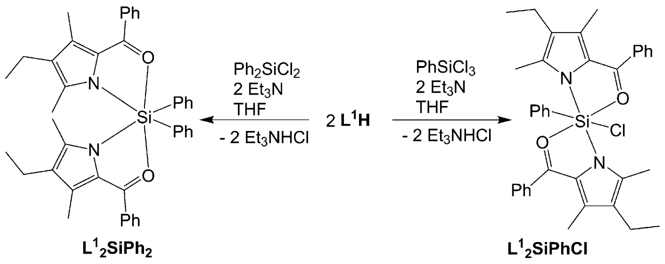

Scheme 4. Base-supported syntheses of hexacoordinate phenylsilicon complexes with two chelating 2-benzoylpyrrolide ligands.

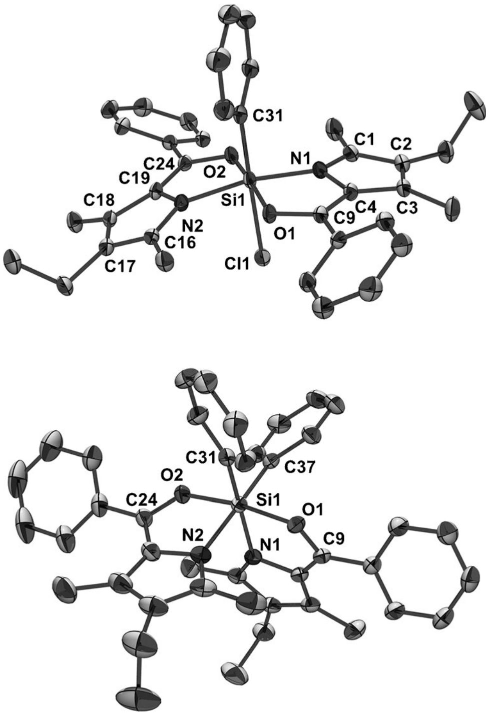

Figure 3. Molecular structures of (from top) **L^1_2SiPhCl** (in the solvate **L^1_2SiPhCl · MeCN**) and **L^1_2SiPh$_2$** in the crystal. Selected atoms are labelled and hydrogen atoms (and solvent molecule from **L^1_2SiPhCl · MeCN**) are omitted for clarity. Selected bond lengths [Å] and angles [°]: **L^1_2SiPhCl**: Si1–Cl1 2.384(1), Si1–O1 1.781(1), Si1–O2 1.791(1), Si1–N1 1.889(1), Si1–N2 1.885(1), Si1–C31 1.926(2), N1–C4 1.411(2), C4–C9 1.388(2), O1–C9 1.320(2); Cl1-Si1-C31 178.7(1), O1-Si1-O2 172.4(1), N1-Si1-N2 168.4(1); **L^1_2SiPh$_2$**: Si1–O1 1.805(1), Si1–O2 1.800(1), Si1–N1 1.980(1), Si1–N2 1.993(1), Si1–C31 1.942(1), Si1–C37 1.937(1); O1-Si1-O2 171.4(1), N1-Si1-C31 171.8(1), N2-Si1-C37 171.9(1), C31-Si1-C37 97.3(1).

requirement would be fulfilled in both the *all-trans* and this particular *cis* configuration, the sterically demanding, and in this compound sterically competing, two Si-bound phenyl groups can gain additional freedom in this *cis*-configuration by forcing the bidentate ligands into the same opposite hemisphere of the coordination sphere. Thus, the sum of the four C-Si-X *cis* angles of each phenyl group can amount to 372.7 and 371.7° for C31 and C37, respectively, whereas the sum of angles would have to be close to 360° in the highly symmetric *all-trans* configuration. In the case of just one Si-bound phenyl group, that is, in **L^1_2SiPhCl**, the two bidentate ligands can be forced toward the sterically less demanding substituent (Cl), and again the Si-bound phenyl group gains sufficient spatial freedom (sum of *cis* angles C31-Si1-X: 379.2°).

Whereas compounds **L^1_2SiR$_2$** (R = Cl, F, OTf, Ph) reveal silicon hexacoordination in the solid state and do not exhibit sufficient solubility for solution-state ^{29}Si NMR spectroscopic investigation (R = Cl, OTf, Ph) or prove to contain hexacoordinate silicon in the solution state (R = F), compound **L^1_2SiPhCl** shows good solubility and ionic dissociation of the Si–Cl bond in CDCl$_3$ solution (Scheme 5), as indicated by a ^{29}Si NMR shift characteristic of pentacoordinate silicon ($\delta = -109.3$ ppm). The progress of the initial stages of this dissociation, however, is reflected by the solid-state structures of three different solvates of **L^1_2SiPhCl** (THF, toluene, MeCN), which contain the molecules of **L^1_2SiPhCl** in similar conformation but with different Si–Cl bond lengths (THF solvate: 2.311(1) and 2.327(1) Å, toluene solvate 2.340(2) Å, MeCN solvate 2.384(1) Å; for the molecular structures see the Supporting Information). For the solution state we have investigated the temperature dependence of the ionic dissociation of **L^1_2SiPhCl** by variable-temperature ^{29}Si NMR spectroscopy in the temperature range 223–316 K. At low temperatures (306 K and below) the ^{29}Si NMR signal appears at $\delta = -105.1$ ppm, thus representing the shift of the pentacoordinate Si atom in the cation **L^1_2SiPh$^+$**. At higher temperatures the signal is shifted to higher field (e.g., $\delta = -111.2$ ppm at 316 K). This counter-intuitive temperature dependence (ionic dissociation upon cooling) has already been reported by Kost et al.[3b] for complexes of the type (*O,N*)$_2$SiPhCl (where (*O,N*) is a mono-anionic hydrazide-derived chelating ligand), and can be attributed to better anion solvation at lower temperatures. For the dissociation of **L^1_2SiPhCl** into **L^1_2SiPh$^+$** and Cl$^-$ we have derived $\Delta H = -39.2$ kJ mol^{-1} and $\Delta S = -122.4$ J mol^{-1} K^{-1} from a linearized LN(K) versus 1/*T* plot (see the Supporting Information). The use of GaCl$_3$ as an efficient chloride scavenger gave rise to the preparation of the salt **[L^1_2SiPh][GaCl$_4$]**, which contains the cationic pentacoordinate silicon complex **[L^1_2SiPh]$^+$** both in CDCl$_3$ solution (δ^{29}Si = −104.6 ppm) and in the solid state (Figure 4, CP/MAS $\delta_{iso}{}^{29}$Si = −105.4 ppm).

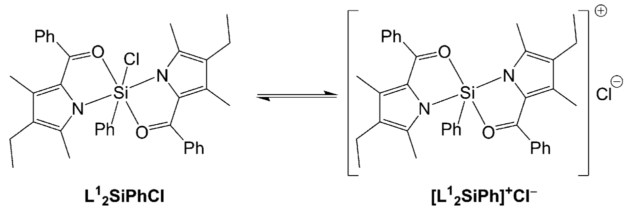

Scheme 5. Ionic dissociation of the Si–Cl bond in **L^1_2SiPhCl**.

The silicon coordination sphere in **[L^1_2SiPh]$^+$** is intermediate between trigonal bipyramidal and square pyramidal, which is reflected by the structural parameter $\tau = 0.53$[15] (derived from the two widest angles of the Si coordination sphere, i.e., the O-Si-O and N-Si-N angles). Lowering of the silicon coordination number results in significant shortening of the Si–N (by

© 2014 Wiley-VCH Verlag GmbH & Co. KGaA, Weinheim

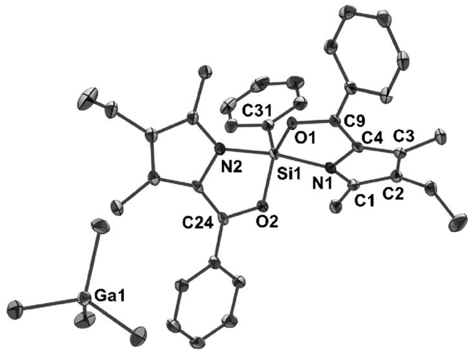

Figure 4. Molecular structure of **[L$^1_2$SiPh][GaCl$_4$]** in the crystal. Selected atoms are labelled and hydrogen atoms are omitted for clarity. Selected bond lengths [Å] and angles [°]: Si1–O1 1.733(2), Si1–O2 1.730(2), Si1–N1 1.874(2), Si1–N2 1.860(2), Si1–C31 1.874(2), N1–C4 1.405(3), C4–C9 1.369(3), O1–C9 1.351(3); O1-Si1-O2 129.9(1), N1-Si1-N2 161.8(1).

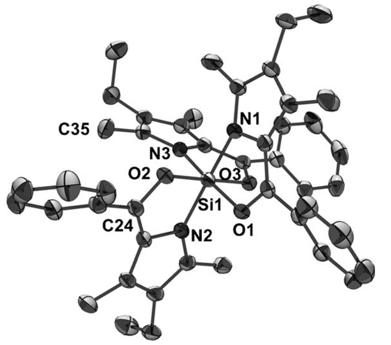

Figure 5. Molecular structure of **[L$^1_3$Si]$^+$** in the crystal structure of **[L$^1_3$Si][GaCl$_4$] · MeCN**. Selected atoms are labelled and hydrogen atoms, anion and solvent molecule are omitted for clarity. Selected bond lengths [Å] and angles [°]: Si1–O1 1.796(1), Si1–O2 1.777(2), Si1–O3 1.780(2), Si1–N1 1.890(2), Si1–N2 1.884(2), Si1–N3 1.863(2); O2-Si1-O3 179.0(1), O1-Si1-N3 173.2(1), N1-Si1-N2 170.0(1).

0.02 Å), Si–C (by 0.05 Å), and Si–O bonds (by 0.05 Å) with respect to the precursor **L$^1_2$SiPhCl**. The predominant shortening of the Si–C and Si–O bonds results from their equatorial positions in **[L$^1_2$SiPh]$^+$** (with respect to a trigonal-bipyramidal Si coordination sphere). The shortening of the Si–O bonds has particular influence on the C–O bonds, which are 0.03 Å longer than in the precursor **L$^1_2$SiPhCl**.

Substitution of the remaining Si–Cl bonds in **L$^1_2$SiCl$_2$** by another **L^1** ligand equivalent (also in this case the use of a sacrificial base is required, and the exact stoichiometry of the base applied is essential, vide infra) affords a cationic silicon (*O*,*N*)-tris-chelate complex with a hexacoordinate Si atom **[L$^1_3$Si]$^+$** (Scheme 6), which could be characterized in the crystal structure of the salt **[L$^1_3$Si][GaCl$_4$]** (Figure 5).

In a CDCl$_3$ solution of the salt **[L$^1_3$Si]Cl**, the ligands give rise to three sets of ^{1}H and ^{13}C NMR signals of equal intensity, and in the ^{29}Si NMR spectrum a sole signal appears at $\delta = -172.6$ ppm. These properties are in accord with the octahedral complex in *mer*-configuration, whereas the *fac*-isomer would comprise three chemically equivalent chelating ligands. This *mer*-configuration of the cation could be confirmed crystallographically in the solid-state structure of **[L$^1_3$Si][GaCl$_4$] · MeCN**. So far, only two kinds of hexacoordinate silicon tris-chelates with three identical (O,N)-bidentate ligands have been characterized crystallographically (**III**[3g] and **IV**[3h]). Whereas the urea-derived compound **III** comprises four-membered chelate rings and *fac*-configuration of the Si coordination sphere, the phenalenyl-derived compound **IV** features six-membered chelate rings and *mer*-configuration of the Si coordination sphere. Thus, the herein reported compound **[L$^1_3$Si][GaCl$_4$] · MeCN** is the first crystallographically characterized silicon tris-chelate of that kind which comprises five-membered chelate rings. For the cationic tris-oxinato silicon complex,[16] which also comprises five-membered chelate rings, we also found *mer*-configuration of the Si coordination sphere, but crystallographic evidence for this configuration in the solid state could not be obtained.

As mentioned earlier, the correct stoichiometry of the supporting base applied is crucial for the successful synthesis of the cationic silicon compound **[L$^1_3$Si]$^+$**. Excess base leads to a deprotonation and C–C coupling reaction of two of the chelating ligands (Scheme 6), and the solid-state structure of the cation **[L$^1_3$Si]$^+$** (Figure 5) already exhibits the prerequisite for this reaction. The pyrrole-bound methyl group C35 is in close proximity to the carbonyl C atom C24 of a neighboring chelate ligand (separation C35···C24 3.22 Å), thus deprotonation at C35 and nucleophilic addition to C24 occurs upon treatment with excess base, furnishing a novel (O,N,O′,N′) tri-anionic tetradentate ligand as confirmed crystallographically in compound **L^{1}L′Si** (Figure 6).

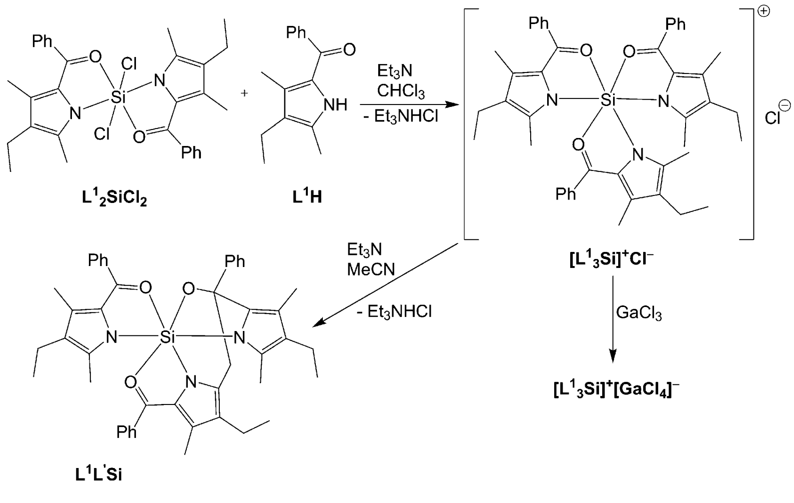

Scheme 6. Synthesis of the cationic hexacoordinate silicon-tris-chelate **L$^1_3$Si$^+$** and its interligand C–C coupling upon deprotonation.

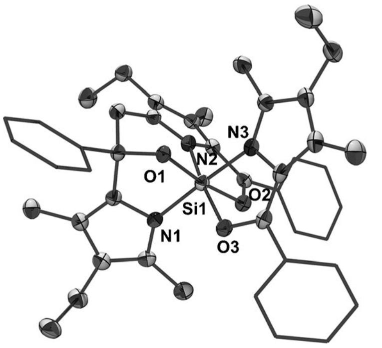

Figure 6. Molecular structure of $\mathbf{L^{1}L'Si}$ in the crystal structure of $\mathbf{L^{1}L'Si \cdot 3\,MeCN}$. Selected atoms are labelled, phenyl groups are shown as stick models, and hydrogen atoms and solvent molecules are omitted for clarity. Selected bond lengths [Å] and angles [°]: Si1–O1 1.717(1), Si1–O2 1.787(1), Si1–O3 1.800(1), Si1–N1 1.826(1), Si1–N2 1.846(1), Si1–N3 1.901(1); O1-Si1-O2 170.2(1), O3-Si1-N2 168.3(1), N1-Si1-N3 171.6(1).

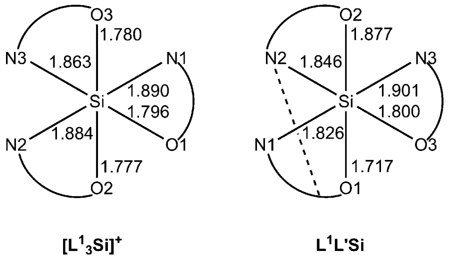

Scheme 7. Schematic representation of corresponding bond lengths [Å] of the Si coordination spheres of the compounds shown in Figure 5 and 6 (atomic labels correspond to Figure 5 and 6 as well). The dashed line indicates the C–C coupling between the two bidentate ligand moieties.

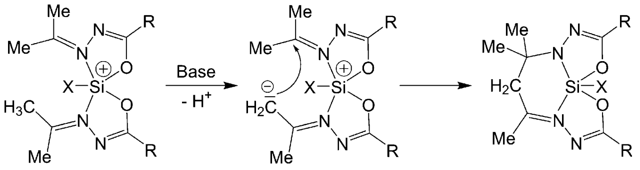

Scheme 8. Inter-ligand C–C coupling under formation of a novel tetradentate ligand from two bidentate (*O*,*N*)-chelators.

Comparison of corresponding bond lengths in the compounds $\mathbf{[L^{1}{}_{3}Si]^{+}}$ and $\mathbf{L^{1}L'Si}$ (Scheme 7) reveals some interesting insights into the coordination behavior of 2-acylpyrrole anions as ligands in general. Whereas in $\mathbf{L^{1}L'Si}$ the rather short Si–O bond to the alkoxy O atom O1 is expected upon ligand coupling (formal transition from a dative to a covalent Si–O bond, Si–O bond length shortening by 0.06 Å upon transition from $\mathbf{[L^{1}{}_{3}Si]^{+}}$ to $\mathbf{L^{1}L'Si}$), basically the same shortening is observed for the Si–N1 bond to the same bidentate ligand moiety. Hence, the originally mono-anionic charge of the bidentate ligand moiety O2N2 in $\mathbf{[L^{1}{}_{3}Si]^{+}}$ (Scheme 7 left) must have been highly delocalized, and upon nucleophilic addition to the carbonyl C atom of this ligand moiety both donor atoms (now O1 and N1 in $\mathbf{L^{1}L'Si}$) have gained from the additional anionic charge to a similar extent. The shorter bond Si1–O1 in $\mathbf{L^{1}L'Si}$ causes a lengthening of the *trans*-disposed Si1–O2 bond and therefore a shift of the delocalized negative charge of this bidentate ligand moiety to the donor atom N2, which thus establishes a shorter bond Si1–N2. The Si–O and Si–N bond lengths within the remaining bidentate ligand moiety (O1N1 in $\mathbf{[L^{1}{}_{3}Si]^{+}}$, O3N3 in $\mathbf{L^{1}L'Si}$) are hardly altered by this transformation of the Si coordination sphere and by the different net charges of the two complexes.

This interligand C–C coupling reaction with formation of $\mathbf{L^{1}L'Si}$ from $\mathbf{[L^{1}{}_{3}Si]^{+}}$ is related to the fusion of two (*O*,*N*)-bidentate ligands observed by Kost et al. (Scheme 8),[17] which also proceeds along the route of deprotonation of an alkyl group in the β-position to an Si-bound N atom and nucleophilic addition of the carbanion to a carbonyl-analogous electrophilic center of a second ligand (i.e., to an imine C atom in this case).

Since three of the five possible octahedral complex configurations (i.e., *all-trans*, *NN-trans*, and *OO-trans* in Scheme 9) have been encountered with our bis-chelate complexes $\mathbf{L^{1}{}_{2}SiX_{2}}$, we analyzed the relative energies of the five isomers for compounds $\mathbf{L^{1}{}_{2}SiCl_{2}}$, $\mathbf{L^{1}{}_{2}SiF_{2}}$, $\mathbf{L^{1}{}_{2}SiPh_{2}}$, and $\mathbf{L^{1}{}_{2}SiPhCl}$ by quantum chemical analyses with Gaussian09,[18] that is, optimization of the molecular geometries for the gas phase (at the DFT MPW1PW91/6-311G(d,p) level) and single-point energy analyses of the local minima (at the MP2/6-311G(d,p) level) (Table 1). (Note: For $\mathbf{L^{1}{}_{2}SiPhCl}$, six isomers were considered due to the chemically non-equivalent positions X and X′ in the *all-cis* isomer.)

For the four compounds under investigation we found an in general pronounced instability of the *XX-trans* isomer. This can be attributed to the two methyl groups in pyrrole-2-position which face each other in this isomer and cause pronounced interligand repulsion. For $\mathbf{L^{1}{}_{2}SiCl_{2}}$ and $\mathbf{L^{1}{}_{2}SiF_{2}}$ the computational analyses confirm the experimentally found configurations as energetic minima that display reasonable energetic difference to the alternative isomers. Interestingly, for $\mathbf{L^{1}{}_{2}SiPh_{2}}$ the *all-cis* isomer is predicted to be slightly more stable than the experimentally encountered configuration, and the *all-trans* isomer is

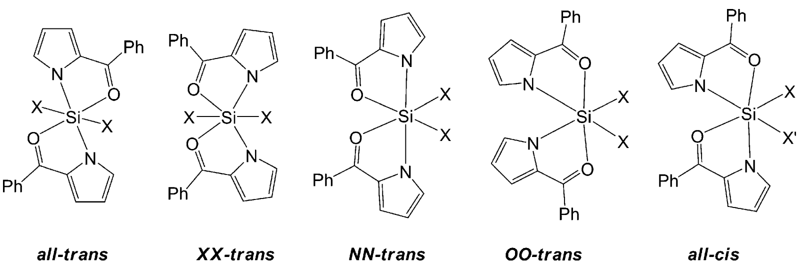

Scheme 9. Different configurational isomers of the hexacoordinate silicon-bis-chelates $\mathbf{L^{1}{}_{2}SiX_{2}}$ analyzed by quantum-chemical calculations (pyrrole-bound alkyl substituents are omitted here for clarity but have been included in the computational analyses).

© 2014 Wiley-VCH Verlag GmbH & Co. KGaA, Weinheim

Table 1. Relative energies [kJ mol^{-1}] of the different octahedral isomers for each of the compounds **$L^1_2SiCl_2$**, **$L^1_2SiF_2$**, **$L^1_2SiPh_2$**, and **$L^1_2SiPhCl$** at the MPW1PW91/6-311G(d,p) level. Relative single-point energies at the MP2/6-311G(d,p) level are given in parentheses. Data corresponding to the experimentally (X-ray) found configuration are given in italics.

Compound	$L^1_2SiCl_2$	$L^1_2SiF_2$	$L^1_2SiPh_2$	$L^1_2SiPhCl$
all-trans	*0.0 (0.0)*	28.9 (30.1)	9.2 (10.5)	*3.8 (9.2)*
XX-trans	51.9 (47.3)	68.2 (63.6)	55.7 (55.3)	55.3 (56.9)
NN-trans	10.9 (8.8)	*0.0 (0.0)*	32.2 (38.5)	0.0 (7.1)
OO-trans	16.8 (1.3)	30.6 (14.7)	*8.8 (8.4)*	5.9 (0.0)
all-cis	17.6 (2.5)	17.6 (7.5)	0.0 (0.0)	8.8 (6.3)[a] 6.7 (5.0)[b]

[a] Cl-*trans*-O, Ph-*trans*-N. [b] Cl-*trans*-N, Ph-*trans*-O.

energetically equivalent to the experimentally found arrangement. Hence, the initial interpretation of the origin of the molecular configuration of **$L^1_2SiPh_2$** has only limited significance, and further contributions such as intermolecular crystal packing effects may play the more important role in this case. For **$L^1_2SiPhCl$** the five isomers *all-trans*, *NN-trans*, *OO-trans*, and *all-cis* exhibit similar relative energies. In this context it is surprising that in the three different crystal structures (three different solvates) of this complex we have found the *all-trans* isomer exclusively. Unfortunately, in both cases, investigation of the coexistence of various isomers in solution (e.g., by variable-temperature solution-state NMR spectroscopy) was hampered by poor solubility (of **$L^1_2SiPh_2$**) or by ionic dissociation (of **$L^1_2SiPhCl$**).

Conclusion and Outlook

In this study we have shown that 2-acylpyrroles can be utilized as mono-anionic *O,N*-chelators in silicon coordination chemistry. Our first examples of silicon complexes synthesized therefrom already indicate both flexibility of those ligands in the Si coordination sphere (arrangement of bis-chelates such as **$L^1_2SiCl_2$**, **$L^1_2SiF_2$** and **$L^1_2SiPh_2$** in various configurations) and reactivities of the ligands which exceed the pure coordination chemistry (Si-templated C–C coupling, high yield of **$L^1_2SiCl_2$** along various syntheses routes such as dehydrogenative coupling of **L^1H** with H_2SiCl_2, and syntheses of cationic silicon complexes by chloride abstraction with $GaCl_3$).

In principle, complexes of the type L_2SiX_2 with L = anion of a 2-acylpyrrole offer various sites for electronic modifications, that is, substituents at the pyrrole backbone, various acyl groups and different monodentate Si-bound substituents X. Further exploration of this interesting system of Si complexes is currently under way.

Experimental Section

Computational Analyses

All quantum-chemical calculations for the geometry optimization (at DFT MPW1PW91 6–311G (d,p) level) and the single-point energy analyses (at MP2 6–31G (d) level) were performed on isolated molecules (gas phase) using Gaussian 09.[18] The Cartesian coordinates of the optimized molecular structures are available in the Supporting Information.

Syntheses and Characterization

General considerations: Most of the starting materials commercially available were used as received without further purification, benzoyl chloride was distilled prior to use. 2,4-Dimethyl-3-ethylpyrrole[19] (kryptopyrrole) was prepared according to a literature procedure. Solvents were distilled from sodium benzophenone (THF and diethyl ether) or sodium (hexane and toluene) or CaH_2 (dichloromethane) and were stored over sodium wire (diethyl ether, hexane, toluene) or activated molecular sieves 3 Å under an argon atmosphere (THF, dichloromethane). Amylene-stabilized chloroform and acetonitrile were received as spectroscopic grade and were stored over activated molecular sieves 3 Å. All reactions were carried out under an atmosphere of dry argon utilizing standard Schlenk techniques. Solution-state ^1H, ^{13}C and ^{29}Si NMR spectra were recorded on a Bruker Avance III 500 MHz spectrometer or on a Bruker DPX 400 spectrometer (Me_4Si as internal standard), solid-state ^{29}Si NMR spectra were recorded on a Bruker Avance^{TM} 400 MHz WB spectrometer in 4 mm ZrO_2 rotors or in 7 mm ZrO_2 rotors with KelF inserts. Elemental analyses were performed by using an Elementar vario MICRO cube. Single-crystal X-ray diffraction data were collected on a STOE IPDS 2/2T single-crystal diffractometer using Mo Kα-radiation. The structures were solved by direct methods using SHELXS-97 and refined by applying the full-matrix least-squares method of F^2 against all reflections with SHELXL-97[20] in WinGX.[21] Graphics of the molecular structures were generated with ORTEP32[22] and POV-RAY.[23] (Color versions of the molecular structures shown in this paper are available in the Supporting Information.) All non-hydrogen atoms were anisotropically refined. C-bound hydrogen atoms were isotropically refined in idealized positions (riding model), N-bound H atoms were located as residual electron density peaks and were refined isotropically. CCDC-993365 (**L^1H**), CCDC-993366 (**L^2H**), CCDC-993377 (**L^3H**), CCDC-993372 (**L^4H**), CCDC-993367 (**$L^1_2SiCl_2$**), CCDC-993375 (**$L^2_2SiCl_2$**), CCDC-993373 (**$L^4_2SiCl_2$**), CCDC-993374 (**$L^1_2SiF_2$·benzene**), CCDC-993369 (**$L^1_2Si(OTf)_2$**), CCDC-993378 (**$L^1_2SiPh_2$**), CCDC-993371 (**$L^1_2SiPhCl$·toluene**), CCDC-993370 (**$L^1_2SiPhCl$·MeCN**), CCDC-993368 (**$L^1_2SiPhCl$·THF**), CCDC-993381 (**[L^1_2SiPh][$GaCl_4$]**), CCDC-993380 (**[L^1_3Si][$GaCl_4$]·MeCN**) and CCDC-993379 (**$L^1(L')Si$·3 MeCN**) contain the supplementary crystallographic data for this paper. These data can be obtained free of charge from The Cambridge Crystallographic Data Centre via www.ccdc.cam.ac.uk/data_request/cif. Selected parameters of data collection and structure refinement are listed in the Supporting Information.

Synthesis of 2-benzoyl-3–5-dimethyl-4-ethyl-1*H*-pyrrole L^1H: To a solution of kryptopyrrole (6.15 g, 50.0 mmol) and Et_3N (7.07 g, 50.30 mmol, excess) in THF (50 mL) at room temperature was added benzoyl chloride (5.19 g, 51.3 mmol, excess) over few minutes. Thereafter the mixture was heated under reflux for 6 h and then cooled to room temperature. The triethylamine hydrochloride precipitate was removed by filtration and was washed with THF (4×5 mL). From the combined filtrate and washings the volatiles were removed in vacuo (trap condensation) and the solid residue was recrystallized from methanol. Yield: 7.82 g (34.40 mmol, 69 %), colorless solid. M.p. 137 °C; ^1H NMR (500 MHz, $CDCl_3$): $\delta = 1.05$ (t, ^3J(H,H) = 7.56 Hz, 3 H, CH_2CH_3), 1.90 (s, 3 H, CH_3), 2.25 (s, 3 H CH_3), 2.38 (q, ^3J(H,H) = 7.56 Hz, 2 H, CH_2CH_3), 7.41–7.52 (m, 3 H, ar), 7.61–7.63 (m, 2 H, ar), 9.09 ppm (s (br.), 1 H, NH); ^{13}C NMR (125 MHz, $CDCl_3$) $\delta = 11.6$ (pyrrole 4 CH_3), 11.7 (pyrrole 2 CH_3), 15.1 (CH_2CH_3), 17.2 (CH_2CH_3), 125.3, 126.9, 128.3, 132.7 (pyrrole ring), 128.2, 128.2,

© 2014 Wiley-VCH Verlag GmbH & Co. KGaA, Weinheim

130.7, 140.5 (phenyl), 185.4 ppm (C=O); elemental analysis (%) calcd for $C_{15}H_{17}NO$: C 79.26, H 7.54, N 6.16; found: C 79.38, H 7.55, N 6.13.

Ligands **L^2H**, **L^3H**, and **L^4H** were synthesized in an analogous manner, for yield and characterization see Supporting Information.

Synthesis of $L^1{}_2SiCl_2$ from $SiCl_4$: To a stirred solution of 2-benzoyl-3,5-dimethyl-4-ethyl-1*H*-pyrrole **L^1H** (1.06 g, 4.66 mmol) in toluene (100 mL) was added $SiCl_4$ (440 mg, 2.56 mmol, 10% excess) dropwise at room temperature, whereupon precipitation of a bright yellow solid commenced. After complete addition of $SiCl_4$, stirring was continued for 1 h. Subsequently, the yellow product was filtered off, washed with toluene (3×5 mL), and dried in vacuo. Yield 1.18 g (2.14 mmol, 92%). Crystals suitable for X-ray analysis were obtained by addition of $SiCl_4$ (70 mg, 0.41 mmol) to a solution of **L^1H** (170 mg, 0.75 mmol) in toluene (75 mL) at 50 °C and leaving the solution undisturbed at this temperature for 7 h. M.p. (sealed capillary, uncorrected) 305 °C (decomp); ^{29}Si CP/MAS NMR (79.5 MHz, $\nu_{spin}=4$ kHz): $\delta_{iso}=-171.0$ ppm; elemental analysis (%) calcd for $C_{30}H_{32}N_2O_2SiCl_2$: C 65.33, H 5.85, N 5.08; found: C 65.35, H 6.02, N 4.91. The compound has very poor solubility in solvents such as chloroform, THF, benzene, toluene, and acetonitrile. In DMSO it undergoes dissociation and formation of a DMSO-solvated silicon complex,[6s] that is **$[L^1{}_2Si(DMSO)_2]^{2+}$**, thus it is soluble in $[D_6]$DMSO and produces the same set of NMR signals as **$L^1{}_2Si(OTf)_2$** does, which thus forms the same complex in DMSO solution. ^1H NMR (400 MHz, $[D_6]$DMSO): $\delta=0.98$ (t, $^3J(H,H)=7.7$ Hz, 6H, CH_2CH_3), 2.18 (s, 6H, CH_3), 2.22 (s, 6H, CH_3), 2.39 (q, $^3J(H,H)=7.7$ Hz, 4H, CH_2CH_3), 7.22 (d, 7.1 Hz, 2H, Si(oPh)), 7.39 (m, 2H, Si(mPh)), 7.49 (m, 1H, Si(pPh)), 7.73 (m, 4H, mPh^L), 7.83 (m, 2H, pPh^L), 8.07 ppm (d, 7.4 Hz, 4H, oPh^L); ^{13}C NMR (100.1 MHz, $[D_6]$DMSO): $\delta=12.4$, 13.3, 13.9, 16.9 (alkyl), 34 (broad multiplet, Si-coordinated $[D_6]$DMSO), 129.1, 129.9, 130.1, 133.8, 133.9, 137.5, 139.0, 158.9, 168.5 ppm (C=O); ^{29}Si NMR (79,5 MHz, $[D_6]$DMSO): $\delta=-175.5$ ppm.

Synthesis of $L^1{}_2SiCl_2$ from $HSiCl_3$: To a stirred solution of **L^1H** (1.00 g, 4.40 mmol) in toluene (100 mL) at 0 °C was added $HSiCl_3$ (300 mg, 2.20 mmol) in one portion. Upon evolution of gas, a bright yellow solid precipitated. The mixture was stirred at 0 °C for 30 min and was then stored at room temperature overnight. Thereupon, the yellow product was filtered off, washed with diethyl ether (3×5 mL) and dried in vacuo. Yield 1.11 g (2.01 mmol, 92%). ^{29}Si CP/MAS NMR (79.5 MHz, $\nu_{spin}=4$ kHz): $\delta_{iso}=-171.0$ ppm; elemental analysis (%) calcd for $C_{30}H_{32}N_2O_2SiCl_2$: C 65.33, H 5.85, N 5.08; found: C 65.09, H 5.82, N 4.96.

Synthesis of $L^1{}_2SiCl_2$ from H_2SiCl_2: To a stirred solution of **L^1H** (1.00 g, 4.40 mmol) in toluene (100 mL) at 0 °C was added 555 mg of a H_2SiCl_2 solution in toluene (40% w/w H_2SiCl_2, 2.20 mmol). Soon after the addition, gas evolution commenced and a bright yellow solid precipitated. The mixture was stirred at 0 °C for 2 h and was then stored at room temperature overnight. Thereupon, the yellow product was filtered off, washed with diethyl ether (3×5 mL) and dried in vacuo. Yield 1.06 g (1.91 mmol, 87%). ^{29}Si CP/MAS NMR (79.5 MHz, $\nu_{spin}=5$ kHz): $\delta_{iso}=-171.0$ ppm; elemental analysis (%) calcd for $C_{30}H_{32}N_2O_2SiCl_2$: C 65.33, H 5.85, N 5.08; found: C 65.61, H 5.84, N 5.04.

Compounds **$L^2{}_2SiCl_2$**, **$L^3{}_2SiCl_2$** and **$L^4{}_2SiCl_2$** were synthesized from $SiCl_4$ as described for **$L^1{}_2SiCl_2$**. For yield and characterization see Supporting Information.

Synthesis of $L^1{}_2SiF_2$: To a suspension of **$L^1{}_2SiCl_2$** (410 mg, 0.743 mmol) in dichloromethane (25 mL) was added ZnF_2 (155 mg, 1.50 mmol). Upon stirring at room temperature the initially colourless liquid turned yellow within 5 min. Stirring was continued for 1 h. After standing overnight the mixture was filtered through diatomaceous earth, washed with dichloromethane (2×1 mL), and the volatiles were evaporated in vacuo from the combined filtrate and washings. Recrystallization of the residue from benzene and decantation of the supernatant afforded **$L^1{}_2SiF_2\cdot C_6H_6$** as a colorless crystalline product (composition according to single-crystal X-ray structure analysis). Yield 274 mg (0.46 mmol, 62%). Upon storage at room temperature the crystalline product loses solvent of crystallization. ^1H NMR (400 MHz, $CDCl_3$): $\delta=1.07$ (t, $^3J(H,H)=7.7$ Hz, 3H, CH_2CH_3); 2.01 (s, 3H, CH_3), 2.41 (q, $^3J(H,H)=7.7$ Hz, 2H, CH_2CH_3), 2.56 (s, 3H, CH_3), 7.38–7.49, 3 H (m.p,), 7.63 ppm (d, 7.9 Hz, 2H, oPh); ^{13}C NMR (100.1 MHz, $CDCl_3$): $\delta=12.2$ (pyrrole CH_3); 13.2 (pyrrole CH_3), 14.5 (CH_2CH_3), 17.7 (CH_2CH_3), 128.0 (Ph o/m); 129.3 (Ph o/m), 131.1 (Ph p), 132.1 (Ph i), 133.0, 133.6, 135.3, 155.2 (pyrrole), 173.6 ppm (C=O); ^{19}F NMR (376.5 MHz, $CDCl_3$): $\delta=-125.3$ ppm (s, ^{29}Si satellites $^1J(Si\text{-}F)=181$ Hz); ^{29}Si NMR (79.5 MHz, $CDCl_3$): $\delta=-170.9$ ppm (t, $^1J(Si,F)=181$ Hz); ^{29}Si CP/MAS (79.5 MHz, $\nu_{spin}=5$ kHz): $\delta_{iso}=-170.0$ ppm (for signal shape see Supporting Information); elemental analysis (%) calcd for $C_{30}H_{32}N_2O_2SiF_2\cdot 0.25C_6H_6$: C 70.30, H 6.27, N 5.21; found: C 70.20, H 6.55, N 5.50.

Synthesis of $L^1{}_2Si(OTf)_2$: To a suspension of **$L^1{}_2SiCl_2$** (180 mg, 0.326 mmol) in MeCN (10 mL) was added Me_3SiOTf (220 mg, 0.99 mmol, 3 equiv) in one portion at 80 °C. The resulting clear solution was stored undisturbed at room temperature whereupon a yellow solid began to crystallize after 1 h. After leaving the mixture undisturbed overnight the supernatant liquid was removed by decantation and the remaining yellow solid was washed with two portions of MeCN (2×1 mL). Yield 131 mg (0.168 mmol, 52%). M.p. (sealed capillary, uncorrected) 235 °C (decomp); ^{29}Si CP/MAS (79.5 MHz, $\nu_{spin}=10$ kHz): $\delta_{iso}=-175.1$ ppm; elemental analysis (%) calcd for $C_{32}H_{32}N_2O_8SiS_2F_2$: C 49.35, H 4.14, N 3.60, S 8.23; found: C 49.37, H 4.15, N 3.68, S 8.44. Solution NMR spectroscopy (^1H, ^{13}C, ^{29}Si) was possible only in $[D_6]$DMSO and produced the same signals as **$L^1{}_2SiCl_2$**.

Synthesis of $L^1{}_2SiPhCl$: To a solution of **L^1H** (1.15 g, 5.00 mmol) and Et_3N (550 mg, 5.50 mmol) in MeCN (75 mL) was added $PhSiCl_3$ (525 mg, 2.50 mmol) at room temperature in one portion, whereupon a yellow-colored solution resulted from which, after initial stirring was discontinued, a yellow crystalline solid precipitated upon storage at 5 °C for 6 h. The supernatant liquid was decanted off and the yellow solid was washed with three portions of MeCN and, subsequently, dried in vacuo. Yield 783 mg (1.23 mmol, 50%) of **$L^1{}_2SiPhCl\cdot MeCN$**. ^1H NMR (400 MHz, $CDCl_3$): $\delta=1.13$ (t, $^3J(H,H)=7.7$ Hz, 6H, CH_2CH_3), 2.33 (s, 6H, CH_3), 2.39 (s, 6H, CH_3), 2.51 (q, $^3J(H,H)=7.7$ Hz, 4H, CH_2CH_3), 7.22 (d, $^3J(H,H)=7.1$ Hz, 2H, Si(oPh)), 7.39 (m, 2H, Si(mPh)), 7.49 (m, 1H, Si(pPh)), 7.66 (m, 4H, mPh^L), 7.74 (m, 2H, pPh^L), 7.89 ppm (d, $^3J(H,H)=7.5$ Hz, 4H, oPh^L); ^{13}C NMR (100.1 MHz, $CDCl_3$): $\delta=13.1$, 14.1, 14.9, 17.9 (alkyl), 128.9, 129.3 (o/mPh^L), 129.5, 130.1 (o/mPh^L), 131.5, 134.0, 134.4, 135.0, 139.7, 141.5, 162.8 (Ph^L, Ph^{Si}, pyrrole), 168.9 ppm (C=O); ^{29}Si NMR (79,5 MHz, $CDCl_3$): $\delta=-109.3$ ppm; ^{29}Si CP/MAS (79.5 MHz, $\nu_{spin}=5$ kHz): $\delta_{iso}=-156.9$; elemental analysis calcd (%) for $C_{36}H_{37}N_2O_2SiCl\cdot MeCN$: C 71.96, H 6.36, N 6.62; found: C 72.05, H 6.34, N 6.37.

Synthesis of $[L^1{}_2SiPh][GaCl_4]$: To a solution of $GaCl_3$ (55 mg, 0.31 mmol) in $CHCl_3$ (1 mL) was given **$L^1{}_2SiPhCl\cdot MeCN$** (200 mg, 0.31 mmol) as a solid. Upon diffusion of pentane into the resulting greenish yellow solution, a crystalline solid was obtained within three days. The solvent was decanted off, the remaining yellow solid was washed with $CHCl_3$/hexane 2:1 (v/v) (1.5 mL), and dried in vacuo. Yield 210 mg (0.27 mmol, 87%). M.p. (sealed capillary, uncorrected) 260 °C (decomp.); ^1H NMR (400 MHz, $CDCl_3$): $\delta=1.13$ (t, $^3J(H,H)=7.7$ Hz, 6H, CH_2CH_3), 2.33 (s, 6H, CH_3), 2.37 (s, 6H, CH_3), 2.51 (q, $^3J(H,H)=7.7$ Hz, 4H, CH_2CH_3), 7.25 (m, 2H, Si(oPh)), 7.41 (t, $^3J(H,H)=7.2$ Hz, 2H, Si(mPh)), 7.50 (t, $^3J(H,H)=7.2$ Hz, 1H, Si(pPh)),7.65 (t, ^3J(H,H) = 7.4 Hz, 4 H, mPh^L), 7.72 (t, ^3J(H,H) = 7.4 Hz, 2 H, pPh^L), 7.19 ppm (m, 4 H, oPh^L); ^{13}C NMR (100.1 MHz, CDCl$_3$): $\delta =$ 13.1, 14.1, 15.1, 17.9 (alkyl), 129.0, 129.2 (o/mPh^L), 129.3, 130.2 (o/mPh^L), 131.7, 134.2, 134.4, 135.1, 140.1, 141.8, 163.4 (Ph^L, Ph^{Si}, pyrrole), 168.8 ppm (C=O); ^{29}Si NMR (79,5 MHz, CDCl$_3$): $\delta = -104.6$ ppm; ^{29}Si CP/MAS (79.5 MHz, $\nu_{spin} = 5$ kHz): $\delta_{iso} = -105.4$ ppm; elemental analysis calcd (%) for $C_{36}H_{37}N_2O_2SiGaCl_4$: C 56.20, H 4.85, N 3.64; found: C 56.28, H 4.74, N 3.48.

Synthesis of $L^1_2SiPh_2$: This was carried out analogously to that of **$L^1_2SiPhCl$** starting from **L^1H** (170 mg, 0.750 mmol), Et$_3$N (80 mg, 0.80 mmol), and Ph$_2$SiCl$_2$ (100 mg, 0.400 mmol) using MeCN (25 mL) as solvent. Crystallization of the product commenced after 2 h of undisturbed storage at room temperature. After one day the supernatant solvent was decanted off, the remaining yellow solid was washed with MeCN (3×1 mL), and it was dried in vacuo. Yield 173 mg (0.27 mmol, 72%). M.p. (sealed capillary, uncorrected) 246 °C (decomp); ^{29}Si CP/MAS (79.5 MHz, $\nu_{spin} = 5$ kHz): $\delta_{iso} = -159.9$ ppm; elemental analysis calcd (%) for $C_{42}H_{42}N_2O_2Si$: C 79.46, H 6.67, N 4.41; found: C 79.75, H 6.60, N 4.32. This compound has very poor solubility in solvents such as chloroform, DMSO, THF, benzene, toluene, and acetonitrile. Therefore, only solid-state characterization methods were applied.

Synthesis of $[L^1_3Si][GaCl_4]$: To a suspension of **$L^1_2SiCl_2$** (220 mg, 0.40 mmol) in CHCl$_3$ (3 mL) was added a solution of **L^1H** (90 mg, 0.40 mmol) and Et$_3$N (40 mg, 0.40 mmol) in CHCl$_3$ (2 mL). Upon stirring for 5 h an almost clear solution resulted, which was filtered. After washing the filter residue with CHCl$_3$ (2 mL) the combined filtrate and washings were evaporated to dryness and the residue was dissolved in MeCN (1.5 mL). This solution was added to a solution of GaCl$_3$ (70 mg, 0.40 mmol) in THF (0.5 mL) (layering of the MeCN phase over the THF solution was intended, but layering failed). The resulting solution was stored at −20 °C for three days to initialize crystallization, which then proceeded at room temperature and afforded a yellow crystalline solid, which was isolated by decantation and washed with THF (3×0.1 mL) and dried in vacuo. Yield of **$[L^1_3Si][GaCl_4]\cdot 0.5$ MeCN**: 195 mg, 0.21 mmol (53%). ^{1}H NMR (400 MHz, CDCl$_3$): $\delta = 1.00$–1.08 (m, 9 H, CH$_2$CH$_3$), 1.56 (s, 3 H, CH$_3$), 2.01 (s, 3 H, CH$_3$); 2.12 (s, 3 H, CH$_3$), 2.16 (s, 3 H, CH$_3$), 2.27 (s, 3 H, CH$_3$), 2.33 (s, 3 H, CH$_3$), 2.35–2.50 (m, 6 H, CH$_2$CH$_3$), 7.51–7.78 ppm (m, 15 H, aromatic); ^{13}C NMR (100.1 MHz, CDCl$_3$): $\delta = 11.0$, 12.7, 12.9, 13.1, 14.0, 14.2, 14.2, 14.4, 14.4, 17.7, 17.8, 17.9 (alkyl), 128.5, 128.8, 129.0, 129.6, 129,9, 129,9, 131.0, 131.2, 132.8, 133.3, 133.8, 134.3, 134.4, 135.0, 135.3, 136.1, 136.5, 137.3, 137.6, 139.0, 140.0, 156.0, 157.9, 158.3 (3× Ph^L,3x pyrrole), 170.4, 172.8, 173.6 ppm (C=O); ^{29}Si NMR (79.5 MHz, CDCl$_3$): $\delta = -172.6$ ppm; elemental analysis calcd (%) for $C_{45}H_{48}N_3O_3SiGaCl_4 \cdot 0.5$ MeCN: C 58.84, H 5.31, N 5.22; found: C 59,03, H 5.53, N 5.51.

Synthesis of $L^1(L^{'})Si$: To a suspension of **$L^1_2SiCl_2$** (89 mg, 0.16 mmol) in MeCN (2 mL) was given a solution of **L^1H** (37 mg, 0.16 mmol) and Et$_3$N (40 mg, 0.4 mmol, 2.5 equiv) in MeCN (3 mL). Upon stirring at 80 °C for 1 h the resulting solution turned brownish red. Upon standing at room temperature for one week an orange crystalline solid had formed which was isolated from the mixture by decantation and washing with MeCN (2×0.1 mL), and dried in vacuo. Yield of **$L^1(L^{'})Si \cdot 0.5$ MeCN** : 35 mg, 0.048 mmol (30%). ^{1}H NMR (400 MHz, CDCl$_3$): $\delta = 0.85$ (t, ^3J(H,H) = 7.48 Hz, 3 H, CH$_2$CH$_3$), 0.89 (t, ^3J(H,H) = 7.53 Hz, 3 H, CH$_2$CH$_3$), 1.04 (t, ^3J(H,H) = 7.53 Hz, 3 H, CH$_2$CH$_3$), 1.36 (s, 3 H, CH$_3$), 1.70 (s, 3 H, CH$_3$), 1.97 (s, 3 H, CH$_3$), 2.13 (s, 3 H, CH$_3$), 2.15–2.23 (m, 4 H, CH$_2$CH$_3$), 2.30 (s, 3 H, CH$_3$), 2.40 (q, ^3J(H,H) = 7.48 Hz, 2 H, CH$_2$CH$_3$), 3.50 (d, ^2J(H,H) = 16.38 Hz, 1 H, CHH), 3.61 (d, ^2J(H,H) = 16.38 Hz, 1 H, CHH), 7.14–7.90 ppm (m, 15 H, ar); ^{13}C NMR (100.1 MHz, CDCl$_3$) $\delta = 9.2$, 11.1, 12.4, 12.5, 12.8, 14.4, 15.0, 15.9, 17.6, 17.7, 18.3 (alkyl), 35.4 (pyr-CH$_2$CO(pyr')(Ph)), 76.0 ((pyr-CH$_2$CO(pyr')(Ph)), 108.3, 121.5, 122.3, 126.5, 127.2, 127.7, 128.0, 128.2, 130.0, 130.1, 130.5, 131.3, 131.7, 132.2, 133.0, 133.2, 133.3, 134.4, 135.2, 135.8, 135.9, 147.0, 153.2, 154.2 (24 C pyrrol, phenyl) 172.7, 174.9 ppm (C=O); ^{29}Si NMR (79.5 MHz, CDCl$_3$): $\delta = -167.6$ ppm; elemental analysis calcd (%) for $C_{45}H_{47}N_3O_3Si \cdot 0.5$ MeCN: C 76.05, H 6.73, N 6.75; found: C 76.02, H 6.55, N 6.50.

Acknowledgements

This work was performed within the Cluster of Excellence “Structure Design of Novel High-Performance Materials via Atomic Design and Defect Engineering (ADDE)” that is financially supported by the European Union (European regional development fund) and by the Ministry of Science and Art of Saxony (SMWK).

Keywords: chelating ligands · coordination chemistry · hexacoordination · hypercoordination · isomerism · silicon

[1] For reviews on hypercoordinate silicon compounds see, for example: a) J. Wagler, U. Böhme, E. Kroke in *Structure and Bonding, Vol. 155* (Ed.: D. Scheschkewitz), Springer, **2014**, pp. 29–105; b) W. Levason, G. Reid, W. Zhang, *Coord. Chem. Rev.* **2011**, *255*, 1319–1341; c) D. Kost, I. Kalikhman, *Acc. Chem. Res.* **2009**, *42*, 303–314; d) R. Tacke, O. Seiler in *Silicon Chemistry*, (Eds.: P. Jutzi, U. Schubert), Wiley-VCH, Weinheim, **2003**, pp. 324–337; e) C. Chuit, R. J. P. Corriu, C. Reye in *Chemistry of Hypervalent Compounds*, (Ed.: K. Akiba), Wiley-VCH, Weinheim, **1999**, pp. 81–146; f) D. Kost, I. Kalikhman in *The Chemistry of Organo Silicon Compounds, Vol. 2*, (Eds.: Z. Rappoport, Y. Apeloig), John Wiley & Sons Ltd, Chichester, **1998**, pp. 1339–1445.

[2] For recent contributions on hypercoordinate silicon chemistry see, for example: a) J. Weiß, K. Sinner, J. A. Baus, C. Burschka, R. Tacke, *Eur. J. Inorg. Chem.* **2014**, 475–483; b) J. Weiß, B. Theis, J. A. Baus, C. Burschka, R. Bertermann, R. Tacke, *Z. Anorg. Allg. Chem.* **2014**, *640*, 300–309; c) S. Jähnigen, E. Brendler, U. Boehme, G. Heide, E. Kroke, *New J. Chem.* **2014**, *38*, 744–751; d) B. M. Kraft, W. W. Brennessel, *Organometallics* **2014**, *33*, 158–171; e) M. Sohail, R. Panisch, A. Bowden, A. R. Bassindale, P. G. Taylor, A. A. Korlyukov, D. E. Arkhipov, L. Male, S. Callear, S. J. Coles, M. B. Hursthouse, R. W. Harrington, W. Clegg, *Dalton Trans.* **2013**, *42*, 10971–10981; f) M. Sohail, A. R. Bassindale, P. G. Taylor, A. A. Korlyukov, D. E. Arkhipov, L. Male, s. J. Coles, M. B. Hursthouse, R. W. Harrinton, W. Clegg, *Organometallics* **2013**, *32*, 1721–1731; g) F. Bitto, K. Kraushaar, U. Boehme, E. Brendler, J. Wagler, E. Kroke, *Eur. J. Inorg. Chem.* **2013**, 2954–2962; h) J. Wagler, E. Brendler, T. Heine, L. Zhechkov, *Chem. Eur. J.* **2013**, *19*, 14296–14303; i) E. Wächtler, R. Gericke, S. Kutter, E. Brendler, J. Wagler, *Main Group Met. Chem.* **2013**, *36*, 181–191; j) R. Singh, R. Mutneja, V. Kaur, J. Wagler, E. Kroke, *J. Organomet. Chem.* **2013**, *698*, 186–191; k) J. A. Baus, C. Burschka, R. Bertermann, C. F. Guerra, F. M. Bickelhaupt, R. Tacke, *Inorg. Chem.* **2013**, *52*, 10664–10676; l) N. Kano, K. Yanaizumi, X. Meng, N. Havare, T. Kawashima, *Chem. Commun.* **2013**, *49*, 10373–10375; m) U. Böhme, S. Fels, *Inorg. Chim. Acta* **2013**, *406*, 251–255; n) R. Azhakar, R. S. Ghadwal, H. W. Roesky, R. A. Mata, H. Wolf, R. Herbst-Irmer, D. Stalke, *Chem. Eur. J.* **2013**, *19*, 3715–3720; o) Y. Xiong, S. Yao, M. Driess, *Z. Naturforsch. B* **2013**, *68*, 445–452; p) S. Schlecht, M. Finze, R. Bertermann, W. Frank, A. Domann, M. Braun, *Eur. J. Inorg. Chem.* **2013**, 1488–1492; q) A. D. Vasiliev, E. A. Zel'bst, A. S. Soldatenko, Y. I. Bolgova, O. M. Trofimova, M. G. Voronkov, *Struct. Chem.* **2013**, *24*, 1001–1005; r) S. Shekar, S. N. Brown, *Organometallics* **2013**, *32*, 556–564; s) P. P. Samuel, A. P. Singh, S. P. Sarish, J. Matussek, I. Objartel, H. W. Roesky, D. Stalke, *Inorg. Chem.* **2013**, *52*, 1544–1549; t) R. Azhakar, H. W. Roesky, H. Wolf, D. Stalke, *Z. Anorg. Allg. Chem.* **2013**, *639*, 934–938; u) T. J. N. Kenla, M. D. K. Tatong, F. M. Talontsi, B. Dittrich, H. Frauendorf, H. Laatsch, *Chem. Commun.* **2013**, *49*, 7641–7643; v) K. A. Chernyshev, B. A. Gostevskii, L. B. Krivdin, *Russ. J. Org. Chem.* **2013**, *49*, 832–837; w) K. Kawamoto, H. Akashi, M. Yamasaki, T. Shibahara, *Chem. Lett.* **2013**,

42, 389–391; x) W. Levason, D. Pugh, G. Reid, *Inorg. Chem.* **2013**, *52*, 5185–5193; y) S. A. Vedha, V. Solomon, P. Venuvanalingam, *J. Phys. Chem. A* **2013**, *117*, 3529–3538.

[3] For examples of hypercoordinate silicon compounds featuring *O,N*-bidentate ligands see: a) I. Kalikhman, S. Krivonos, L. Lameyer, D. Stalke, D. Kost, *Organometallics* **2001**, *20*, 1053–1055; b) V. Kingston, B. Gostevskii, I. Kalikhman, D. Kost, *Chem. Commun.* **2001**, 1272–1273; c) J. Wagler, U. Boehme, E. Brendler, G. Roewer, *Organometallics* **2005**, *24*, 1348–1350; d) M. Schley, J. Wagler, G. Roewer, *Z. Anorg. Allg. Chem.* **2005**, *631*, 2914–2918; e) K. Hensen, G. Klebe, *J. Organomet. Chem.* **1981**, *209*, 17–23; f) R. Tacke, R. Bertermann, C. Burschka, S. Dragota, M. Penka, I. Richter, *J. Am. Chem. Soc.* **2004**, *126*, 14493–14505; g) D. Schöne, D. Gerlach, C. Wiltzsch, E. Brendler, T. Heine, E. Kroke, J. Wagler, *Eur. J. Inorg. Chem.* **2010**, 461–467; h) S. K. Pal, M. E. Itkis, F. S. Tham, R. W. Reed, R. T. Oakley, R. C. Haddon, *J. Am. Chem. Soc.* **2008**, *130*, 3942–3951.

[4] For hypercoordinate silicon complexes with pyrrole-derived ligands see: a) D. Gerlach, E. Brendler, T. Heine, J. Wagler, *Organometallics* **2007**, *26*, 234–240; b) D. Gerlach, A. W. Ehlers, K. Lammertsma, J. Wagler, *Z. Naturforsch. B* **2009**, *64*, 1571–1579; c) N. Sakamoto, Ch. Ikeda, M. Yamamura, T. Nabeshima, *J. Am. Chem. Soc.* **2011**, *133*, 4726–4729; d) M. Yamamura, M. Albrecht, M. Albrecht, Y. Nishimura, T. Arai, T. Nabeshima, *Inorg. Chem.* **2014**, *53*, 1355–1360; e) J. A. Cissell, T. P. Vaid, A. L. Rheingold, *J. Am. Chem. Soc.* **2005**, *127*, 12212–12213; f) M. Gouterman, F. P. Schwartz, P. D. Smith, D. Dolphin, *J. Chem. Phys.* **1973**, *59*, 676–690; g) K. M. Kane, F. R. Lemke, J. L. Petersen, *Inorg. Chem.* **1995**, *34*, 4085–4091; h) J.-Y. Zheng, K. Konishi, T. Aida, *Inorg. Chem.* **1998**, *37*, 2591–2594.

[5] For complexes with anions of 2-acylpyrroles as ligands see: a) Y. Ding, X. Li, T. Li, W. Zhu, Y. Xie, *J. Org. Chem.* **2013**, *78*, 5328–5338; b) S. Muhammad, V. Yempally, M. Anas, S. Moncho, S. J. Kyran, E. N. Brothers, D. J. Darensbourg, A. A. Bengali, *Inorg. Chem.* **2012**, *51*, 13041–13049; c) T. Lundrigan, C. L. M. Jackson, M. I. Uddin, L. A. Tucker, A. A. Ali, A. Linden, T. S. Cameron, A. Thompson, *Can. J. Chem.* **2012**, *90*, 693–700; d) M. Bröring, R. Krueger, C. Kleeberg, *Z. Anorg. Allg. Chem.* **2008**, *634*, 1555–1559; e) J. Chen, A. Burghart, C.-W. Wan, L. Tai, C. Ortiz, J. Reibenspies, K. Burgess, *Tetrahedron Lett.* **2000**, *41*, 2303–2307; f) K. Huebler, U. Huebler, *Z. Anorg. Allg. Chem.* **2000**, *626*, 1224–1236.

[6] a) D. Schwarz, E. Brendler, E, Kroke, J. Wagler, *Z. Anorg. Allg. Chem.* **2012**, *638*, 1768–1775; b) R. Gericke, D. Gerlach, J. Wagler, *Organometallics* **2009**, *28*, 6831–6834; c) E. Brendler, E. Wächtler, J. Wagler, *Organometallics* **2009**, *28*, 5459–5465; d) J. Wagler, G. Roewer, D. Gerlach, *Z. Anorg. Allg. Chem.* **2009**, *635*, 1279–1287; e) A. Kämpfe, E. Kroke, J. Wagler, *Eur. J. Inorg. Chem.* **2009**, 1027–1035; f) K. Lippe, D. Gerlach, E. Kroke, J. Wagler, *Inorg. Chem. Commun.* **2008**, *11*, 492–496; g) J. Wagler, D. Gerlach, G. Roewer, *Inorg. Chim. Acta* **2007**, *360*, 1935–1942; h) J. Wagler, G. Roewer, *Inorg. Chim. Acta* **2007**, *360*, 1717–1724; i) J. Wagler, *Organometallics* **2007**, *26*, 155–159; j) J. Wagler, E. Brendler, *Z. Naturforsch. B* **2007**, *62*, 225–234; k) J. Wagler, D. Gerlach, G. Roewer, *Chem. Heterocycl. Compd.* **2006**, *474*, 1826–1837; l) J. Wagler, G. Roewer, *Z. Naturforsch. B* **2006**, *61*, 1406–1412; m) J. Wagler, D. Gerlach, U. Böhme, G. Roewer, *Organometallics* **2006**, *25*, 2929–2933; n) J. Wagler, U. Böhme, E. Brendler, B. Thomas, S. Goutal, H. Mayr, B. Kempf, G. Y. Remennikov, G. Roewer, *Inorg. Chim. Acta* **2005**, *358*, 4270–4286; o) J. Wagler, U. Böhme, E. Brendler, S. Blaurock, G. Roewer, *Z. Anorg. Allg. Chem.* **2005**, *631*, 2907–2913; p) J. Wagler, G. Roewer, *Z. Naturforsch. B* **2005**, *60*, 709–714; q) J. Wagler, T. Doert, G. Roewer, *Angew. Chem.* **2004**, *116*, 2495–2498; *Angew. Chem. Int. Ed.* **2004**, *43*, 2441–2444; r) J. Wagler, U. Böhme, G. Roewer, *Organometallics* **2004**, *23*, 6066–6069; s) J. Wagler, U. Böhme, E. Brendler, G. Roewer, *Z. Naturforsch. B* **2004**, *59*, 1348–1352; t) J. Wagler, U. Böhme, G. Roewer, *Angew. Chem.* **2002**, *114*, 1825–1827; *Angew. Chem. Int. Ed.* **2002**, *41*, 1732–1734.

[7] a) J. Autschbach, K. Sutter, L. A. Truflandier, E. Brendler, J. Wagler, *Chem. Eur. J.* **2012**, *18*, 12803–12813; b) F. Bitto, J. Wagler, E. Kroke, *Eur. J. Inorg. Chem.* **2012**, 2402–2408; c) L. A. Truflandier, E. Brendler, J. Wagler, J. Autschbach, *Angew. Chem.* **2011**, *123*, 269–273; *Angew. Chem. Int. Ed.* **2011**, *50*, 255–259; d) J. Wagler, E. Brendler, T. Langer, R. Pöttgen, T. Heine, L. Zhechkov, *Chem. Eur. J.* **2010**, *16*, 13429–13434; e) J. Wagler, E. Brendler, *Angew. Chem.* **2010**, *122*, 634–637; *Angew. Chem. Int. Ed.* **2010**, *49*, 624–627; f) E. Brendler, T. Heine, A. F. Hill, J. Wagler, *Z. Anorg. Allg. Chem.* **2009**, *635*, 1300–1305; g) J. Wagler, A. F. Hill, *Organometallics* **2008**, *27*, 6579–6586; h) J. Wagler, A. F. Hill, *Organometallics* **2007**, *26*, 3630–3632.

[8] A. Kämpfe, E. Kroke, J. Wagler, *Organometallics* **2014**, *33*, 112–120.

[9] a) O. Seiler, M. Büttner, M. Penka, R. Tacke, *Organometallics* **2005**, *24*, 6059–6062; b) R. Bertermann, A. Biller, M. Kaupp, M. Penka, O. Seiler, R. Tacke, *Organometallics* **2003**, *22*, 4104–4110.

[10] a) M. Novák, L. Dostál, M. Alonso, F. De Proft, A. Růžička, A. Lyčka, R. Jambor, *Chem. Eur. J.* **2014**, *20*, 2542–2550; b) K. Lippe, D. Gerlach, E. Kroke, J. Wagler, *Organometallics* **2009**, *28*, 621–629; c) E. Kertsnus-Banchik, I. Kalikhman, B. Gostevskii, Z. Deutsch, M. Botoshansky, D. Kost, *Organometallics* **2008**, *27*, 5285–5294; d) M. Yamamura, N. Kano, T. Kawashima, *Tetrahedron Lett.* **2007**, *48*, 4033–4036.

[11] G. W. Fester, J. Eckstein, D. Gerlach, J. Wagler, E. Brendler, E. Kroke, *Inorg. Chem.* **2010**, *49*, 2667–2673.

[12] K. Junold, C. Burschka, R. Bertermann, R. Tacke, *Dalton Trans.* **2010**, *39*, 9401–9413.

[13] X. Helluy, R. Pietschnig, A. Sebald, *Solid State Nucl. Magn. Reson.* **2003**, *24*, 286–300.

[14] I. Kalikhman, B. Gostevskii, O. Girshberg, S. Krivonos, D. Kost, *Organometallics* **2002**, *21*, 2551–2554.

[15] A. W. Addison, T. N. Rao, J. Reedijk, J. van Rijn, G. C. Verschoor, *J. Chem. Soc. Dalton Trans.* **1984**, 1349–1356.

[16] J. Wagler, M. Schley, D. Gerlach, U. Böhme, E. Brendler, G. Roewer, *Z. Naturforsch. B* **2005**, *60*, 1054–1064.

[17] a) I. Kalikhman, B. Gostevskii, E. Kertsnus, S. Deuerlein, D. Stalke, M. Botoshansky, D. Kost, *J. Phys. Org. Chem.* **2008**, *21*, 1029–1034; b) B. Gostevskii, V. Pestunovich, I. Kalikhman, A. Sivaramakrishna, N. Kocher, S. Deuerlein, D. Leusser, D. Stalke, D. Kost, *Organometallics* **2004**, *23*, 4346–4348.

[18] Gaussian 09, Revision **D.01**, M. J. Frisch, G. W. Trucks, H. B. Schlegel, G. E. Scuseria, M. A. Robb, J. R. Cheeseman, G. Scalmani, V. Barone, B. Mennucci, G. A. Petersson, H. Nakatsuji, M. Caricato, X. Li, H. P. Hratchian, A. F. Izmaylov, J. Bloino, G. Zheng, J. L. Sonnenberg, M. Hada, M. Ehara, K. Toyota, R. Fukuda, J. Hasegawa, M. Ishida, T. Nakajima, Y. Honda, O. Kitao, H. Nakai, T. Vreven, J. A. Montgomery, Jr., J. E. Peralta, F. Ogliaro, M. Bearpark, J. J. Heyd, E. Brothers, K. N. Kudin, V. N. Staroverov, R. Kobayashi, J. Normand, K. Raghavachari, A. Rendell, J. C. Burant, S. S. Iyengar, J. Tomasi, M. Cossi, N. Rega, J. M. Millam, M. Klene, J. E. Knox, J. B. Cross, V. Bakken, C. Adamo, J. Jaramillo, R. Gomperts, R. E. Stratmann, O. Yazyev, A. J. Austin, R. Cammi, C. Pomelli, J. W. Ochterski, R. L. Martin, K. Morokuma, V. G. Zakrzewski, G. A. Voth, P. Salvador, J. J. Dannenberg, S. Dapprich, A. D. Daniels, Ö. Farkas, J. B. Foresman, J. V. Ortiz, J. Cioslowski, and D. J. Fox, Gaussian, Inc., Wallingford CT, **2009**.

[19] A. Treibs, R. Schmidt, *Liebigs Ann. Chem.* **1952**, *577*, 105–115.

[20] a) G. M. Sheldrick, SHELXS-97, A Computer Program for the Solution of Crystal Structures, Version: WinGX©, **1986–1997**, Release 97–2; G. M. Sheldrick, SHELXL97, A Computer Program for Crystal Structure Refinement, Version: WinGX©, 1993–1997, Release 97–2; b) G. M. Sheldrick, *Acta Crystallogr. Sect. A* **2008**, *64*, 112–122.

[21] L. J. Farrugia, WINGX (version 1.64.05), *J. Appl. Crystallogr.* **1999**, *32*, 837–838.

[22] L. J. Farrugia, ORTEP-3 for Windows, *J. Appl. Crystallogr.* **1997**, *30*, 565.

[23] Persistence of Vision Pty. Ltd. Persistence of Vision Raytracer (Version 3.6). Retrieved from http://www.povray.org/download/, **2004**.

Received: March 27, 2014